Supporting Information

Mechanochemical and wet chemical syntheses of CaIn-layered double hydroxide and its performance in a transesterification reaction compared to those of other $Ca_2M(III)$ hydrocalumites (M: Al, Sc, V, Cr, Fe, Ga) and Mg(II)-, Ni(II)-, Co(II)- or Zn(II)-based hydrotalcites

Márton Szabados,[a,b] Anna Adél Ádám[a,b], Péter Traj,[a,b] Szabolcs Muráth,[c,d] Kornélia Baán[e], Péter Bélteky[e], Zoltán Kónya,[e,f] Ákos Kukovecz,[e] Pál Sipos,[b,g] and István Pálinkó[a,b*]

[a]*Department of Organic Chemistry, University of Szeged, Dóm tér 8, Szeged, H-6720 Hungary*
[b]*Material and Solution Structure Research Group, Interdisciplinary Excellence Centre, Institute of Chemistry, University of Szeged, Aradi vértanúk tere 1, Szeged, H-6720 Hungary*
[c]*MTA-SZTE Biocolloids Research Group, Rerrich B. tér 1, Szeged, H-6720, Hungary*
[d]*Interdisciplinary Excellence Centre, Department of Physical Chemistry and Materials Science, University of Szeged, Rerrich B. tér 1, Szeged, H-6720, Hungary*
[e]*Department of Applied and Environmental Chemistry, University of Szeged, Rerrich B. tér 1, Szeged, H-6720 Hungary*
[f]*MTA-SZTE Reaction Kinetics and Surface Chemistry Research Group, Rerrich B. tér 1, Szeged, H-6720 Hungary*
[g]*Department of Inorganic and Analytical Chemistry, University of Szeged, Dóm tér 7, Szeged, H-6720 Hungary*

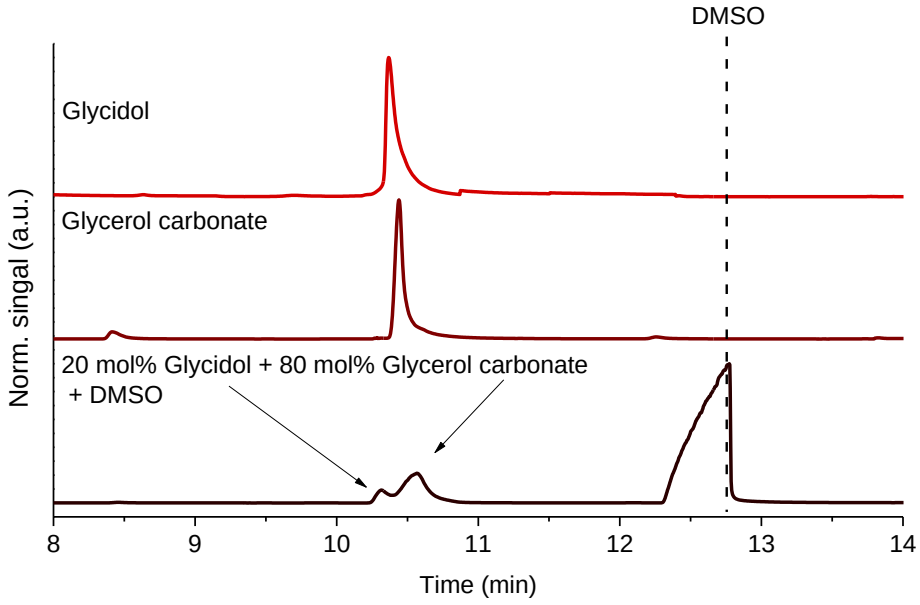

Fig. S1 The advantageous effect of DMSO on the separation of glycidol and glycerol carbonate.

Correponding author: István Pálinkó
E-mail address: palinko@chem.u-szeged.hu (I. Pálinkó)

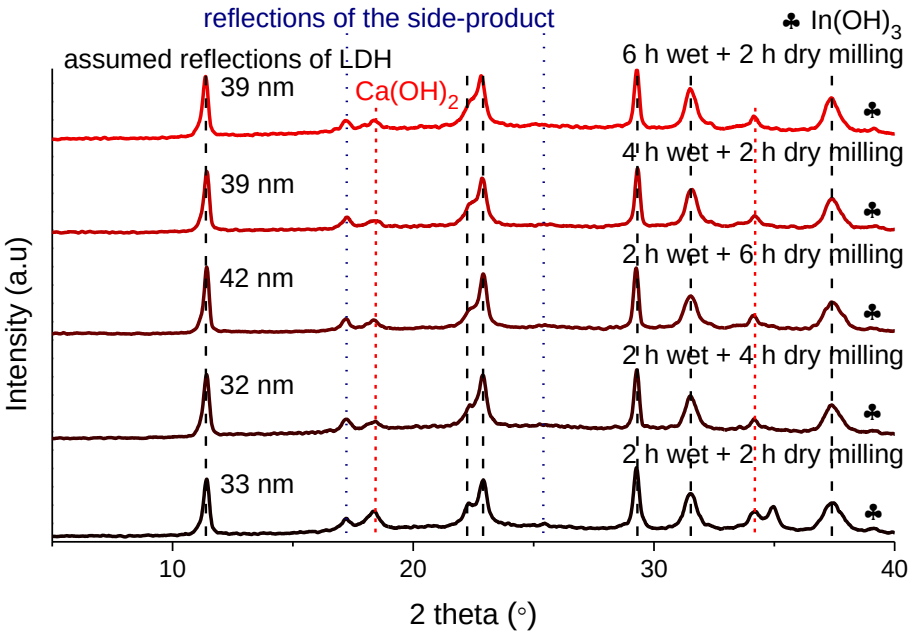

Fig. S2 X-ray powder diffraction patterns for the solids prepared with the purely mechanochemical technique at different wet and dry grinding times (400 µl saturated NaCl solution).

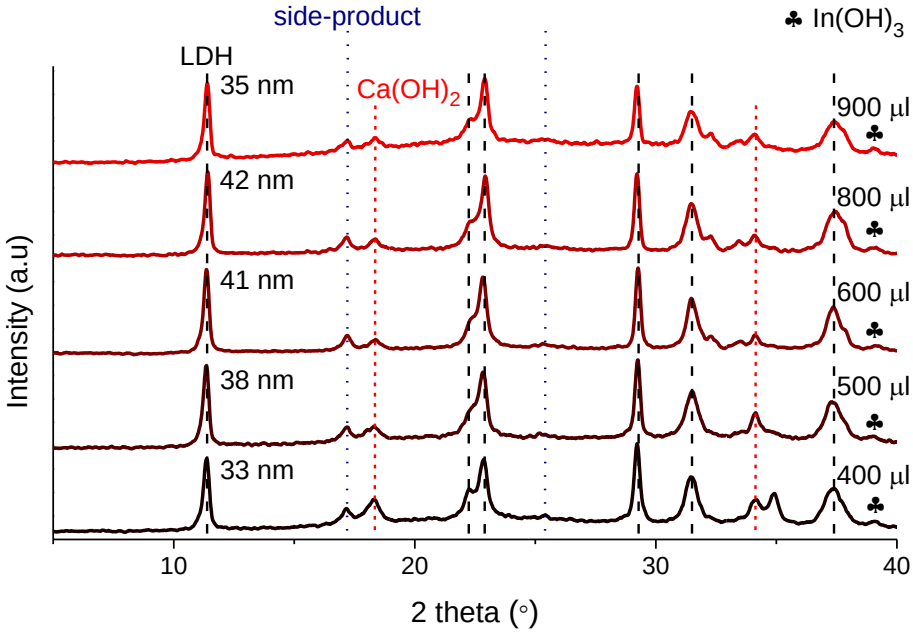

Fig. S3 X-ray powder diffractogram patterns for the samples synthesized by the purely mechanochemical technique at varied amounts of the saturated NaCl solutions (2 h dry and 2 h wet milling).

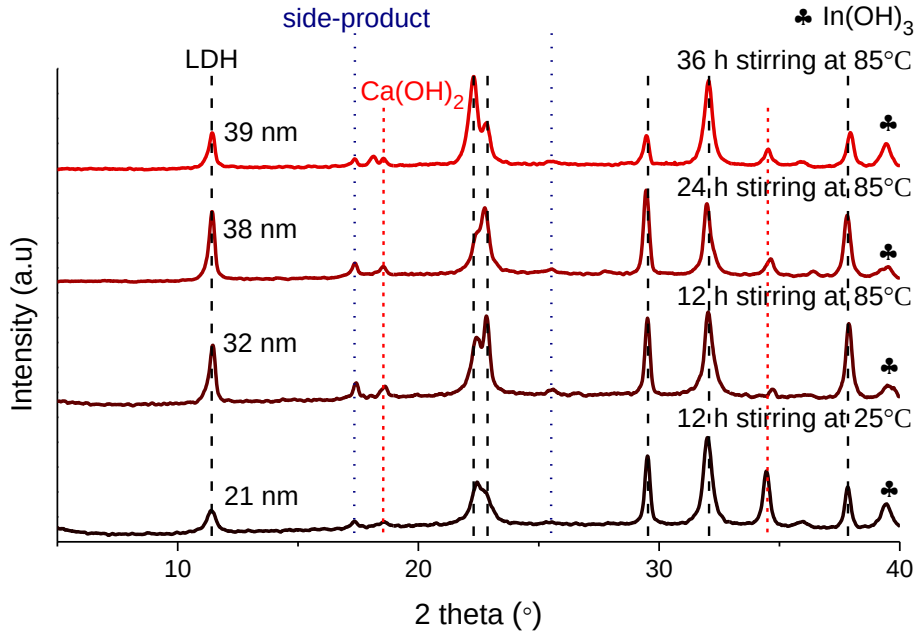

Fig. S4 X-ray powder diffraction patterns for the materials at varied stirring time and temperature prepared by the mechanochemically-aided route (2 h dry grinding, 5 ml 0.4 M NaCl solution).

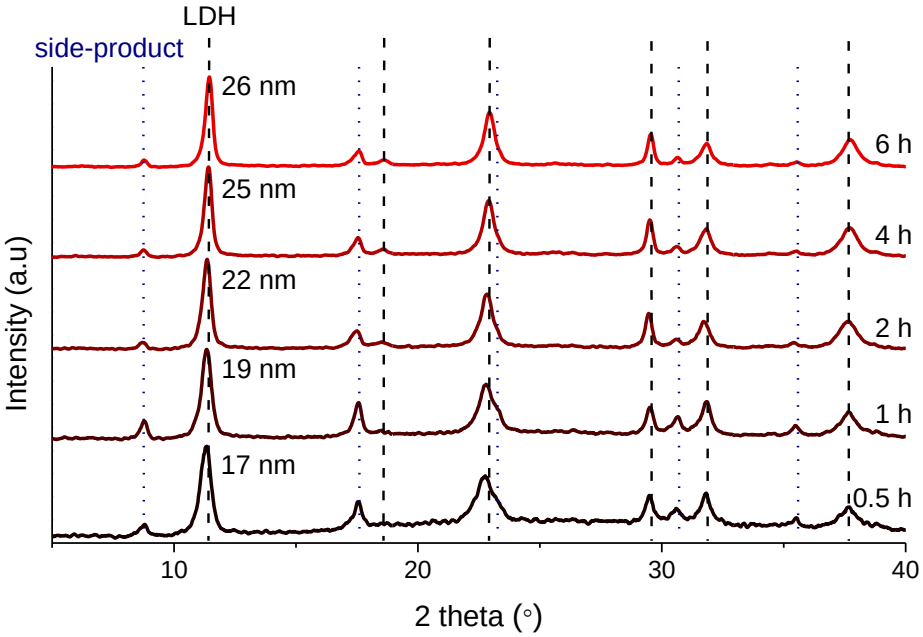

Fig. S5 X-ray powder diffraction patterns for the samples at varying stirring time (room temperature, 2:1 Ca:In initial molar ratio, 3 M base).

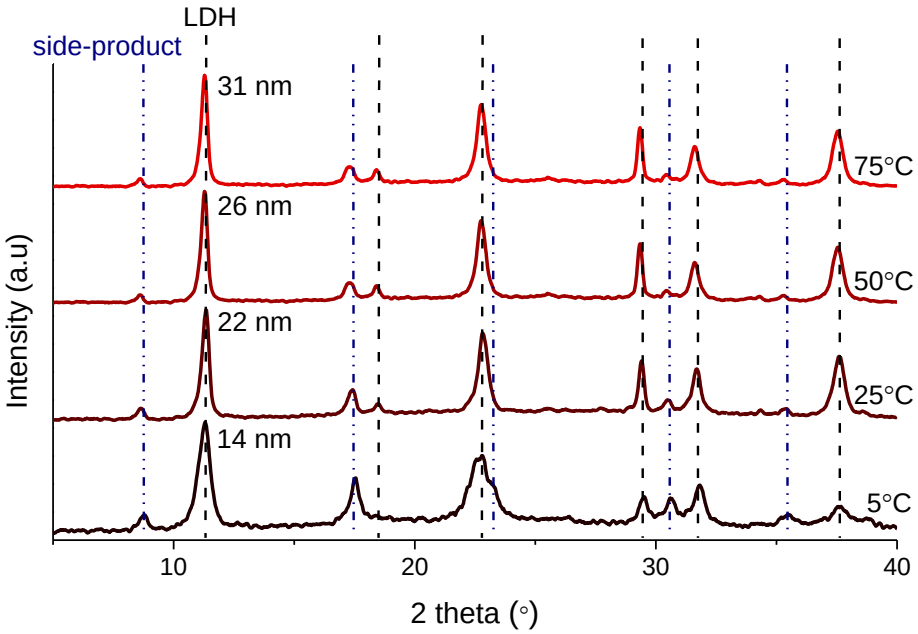

Fig. S6 XRD patterns for the materials prepared at various temperatures (2 h stirring, 2:1 Ca:In initial molar ratio, 3 M base).

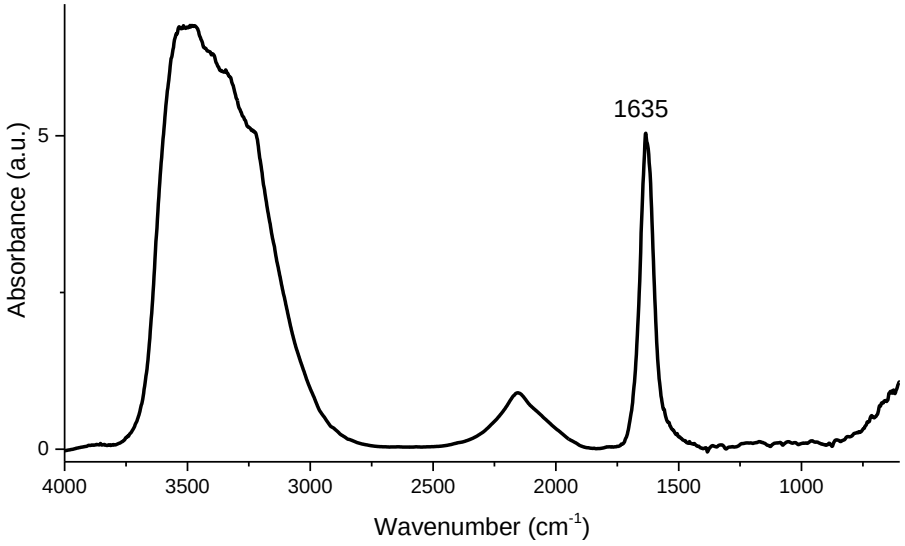

Fig. S7 Infrared spectrum of the $CaCl_2 \times 2H_2O$ starting reagent.

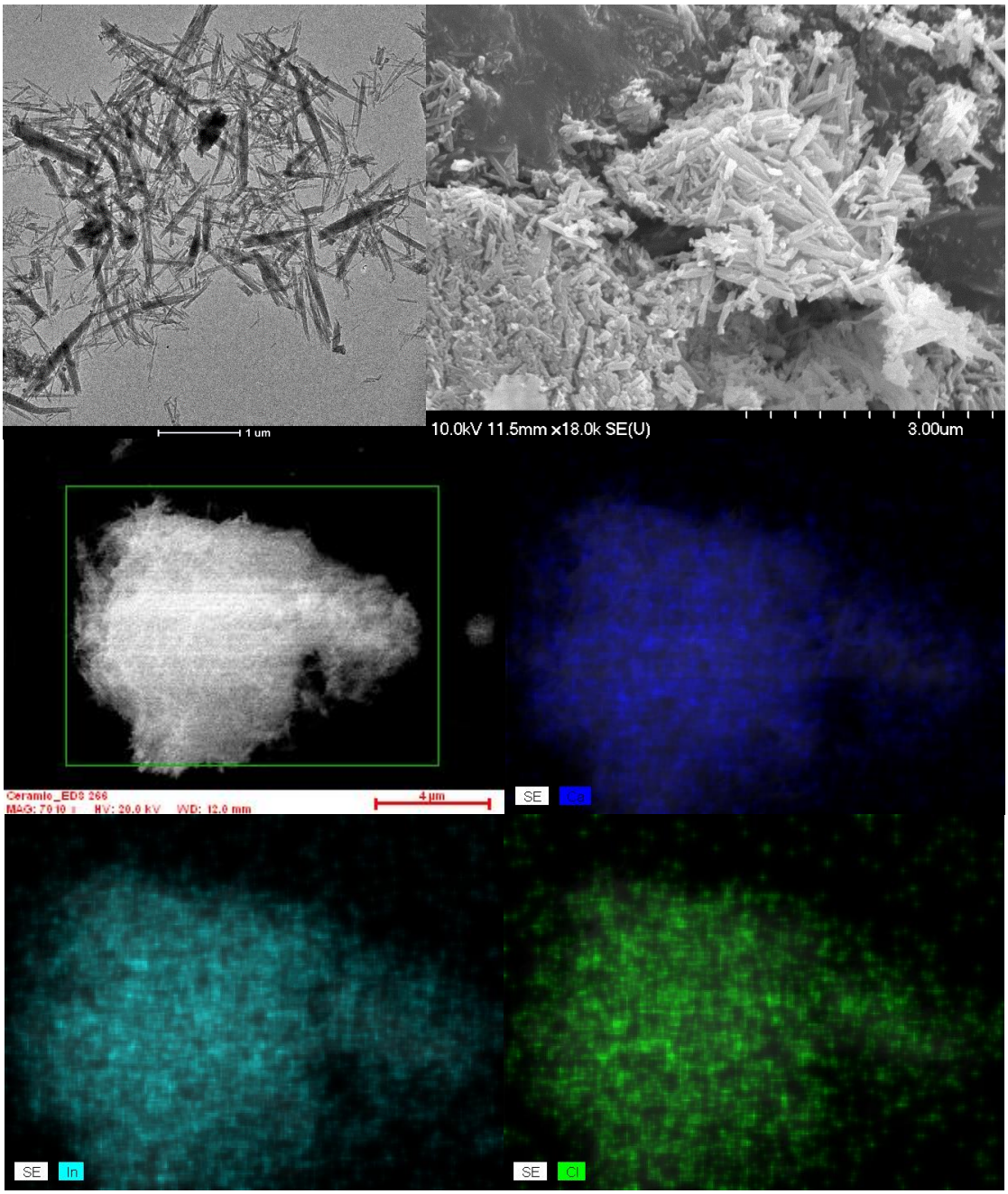

Fig. S8 TEM (the first), SEM (the second) and elemental map (the last four) images for the CaIn-hydroxide-chloride side-product.

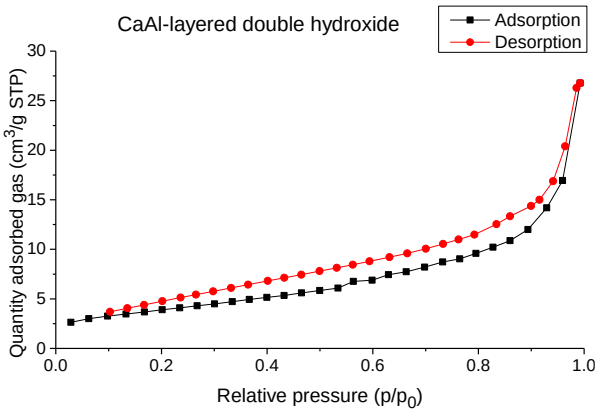
CaAl-layered double hydroxide
Adsorption
Desorption
Quantity adsorbed gas (cm3/g STP)
Relative pressure (p/p0)

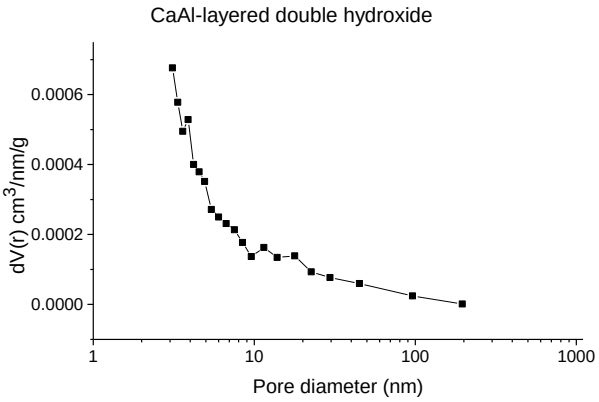
CaAl-layered double hydroxide
dV(r) cm3/nm/g
Pore diameter (nm)

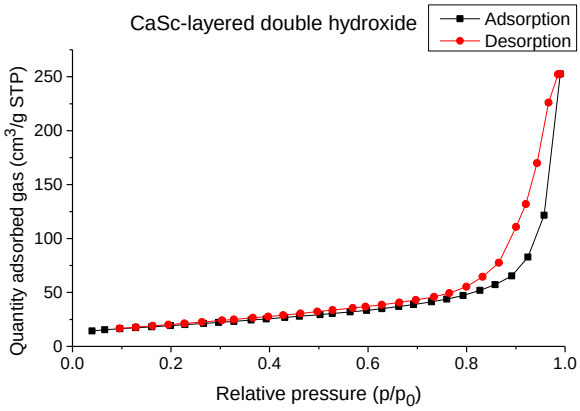
CaSc-layered double hydroxide
Adsorption
Desorption
Quantity adsorbed gas (cm3/g STP)
Relative pressure (p/p0)

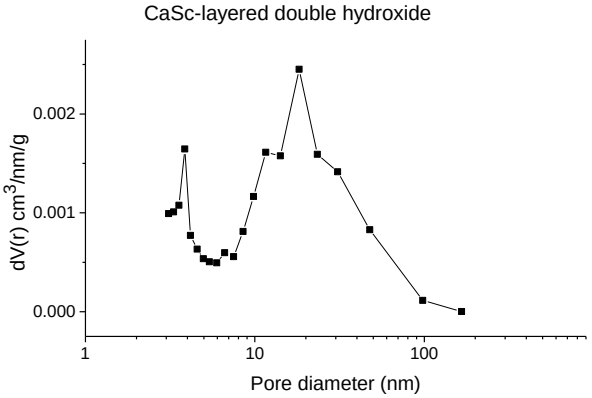
CaSc-layered double hydroxide
dV(r) cm3/nm/g
Pore diameter (nm)

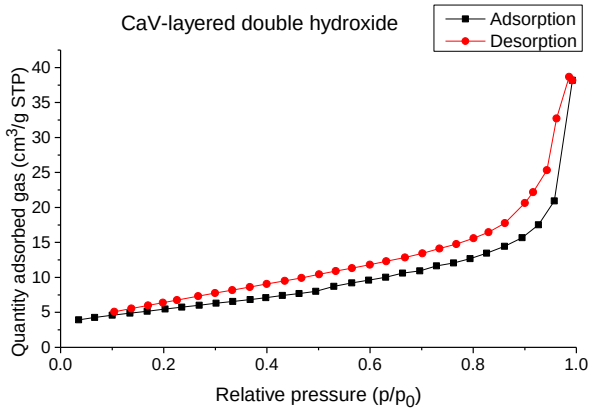
CaV-layered double hydroxide
Adsorption
Desorption
Quantity adsorbed gas (cm3/g STP)
Relative pressure (p/p0)

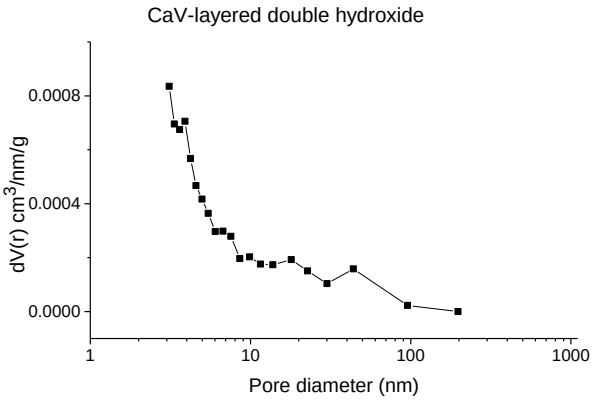
CaV-layered double hydroxide
dV(r) cm3/nm/g
Pore diameter (nm)

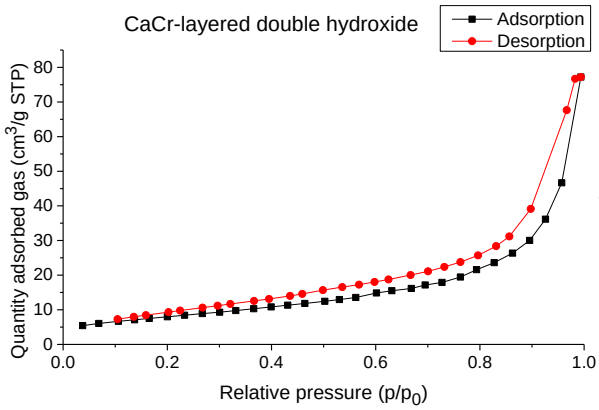
CaCr-layered double hydroxide
Adsorption
Desorption
Quantity adsorbed gas (cm3/g STP)
Relative pressure (p/p0)

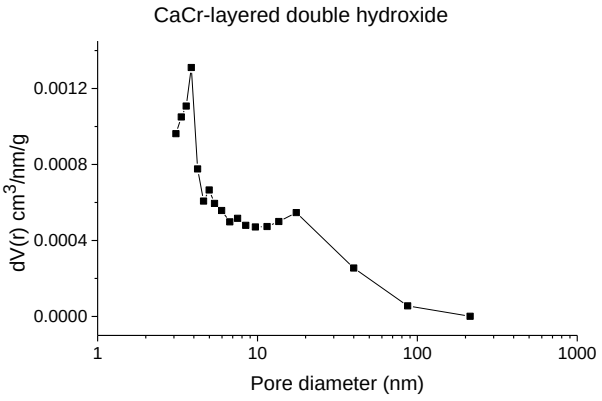
CaCr-layered double hydroxide
dV(r) cm3/nm/g
Pore diameter (nm)

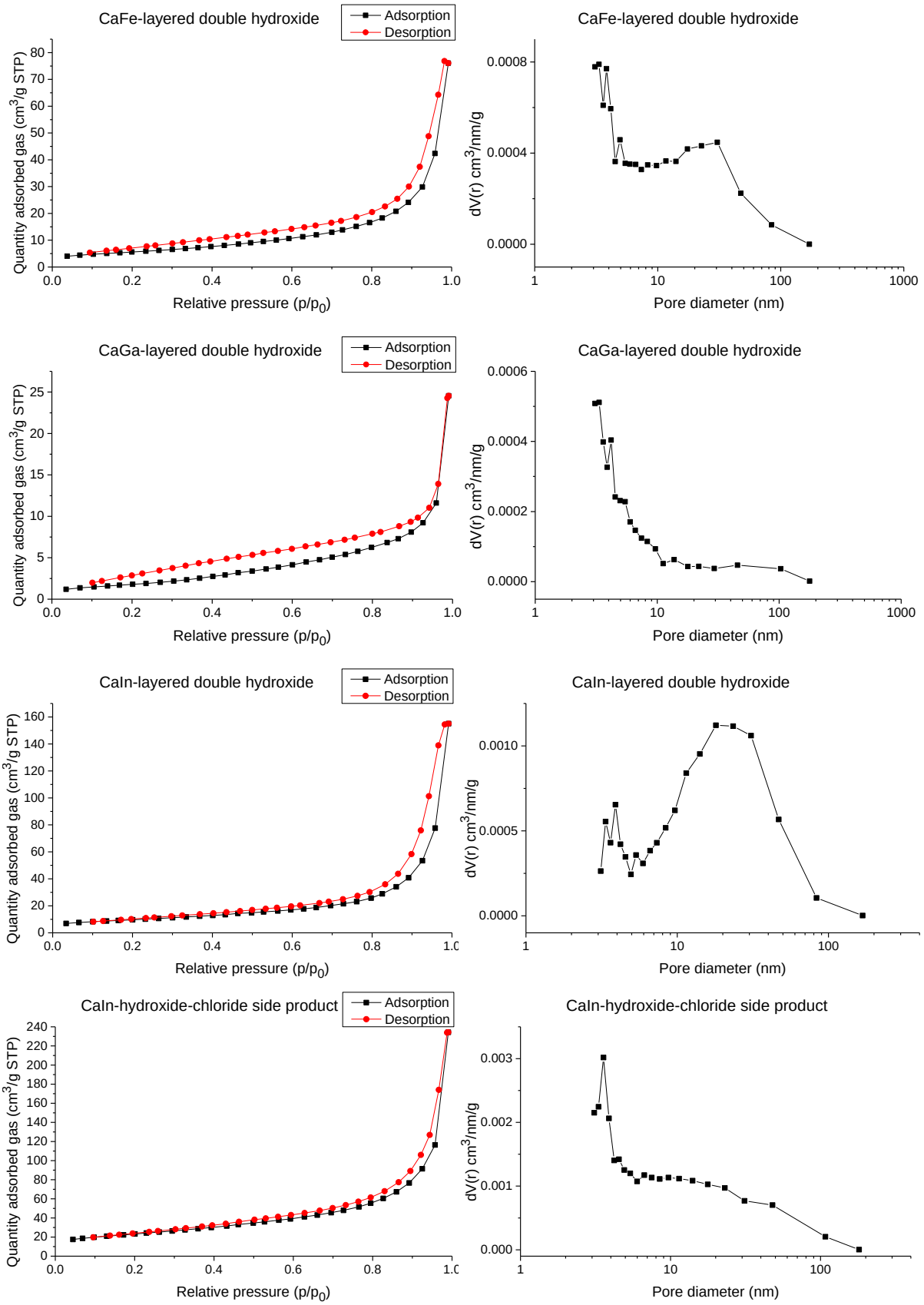

Fig. S9 N_2 adsorption-desorption isotherms (left) and the corresponding pore size distribution plots (right) for the LDHs and the CaIn-hydroxide-chloride side-product.

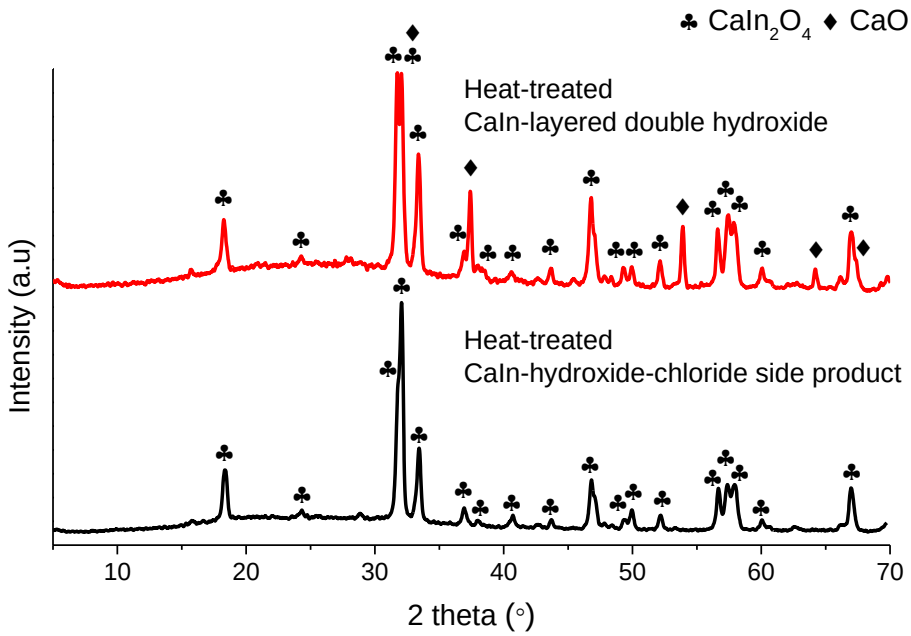

Fig. S10 X-ray powder diffraction patterns for the CaIn-LDH and the side-product after heat treatment at 900°C.

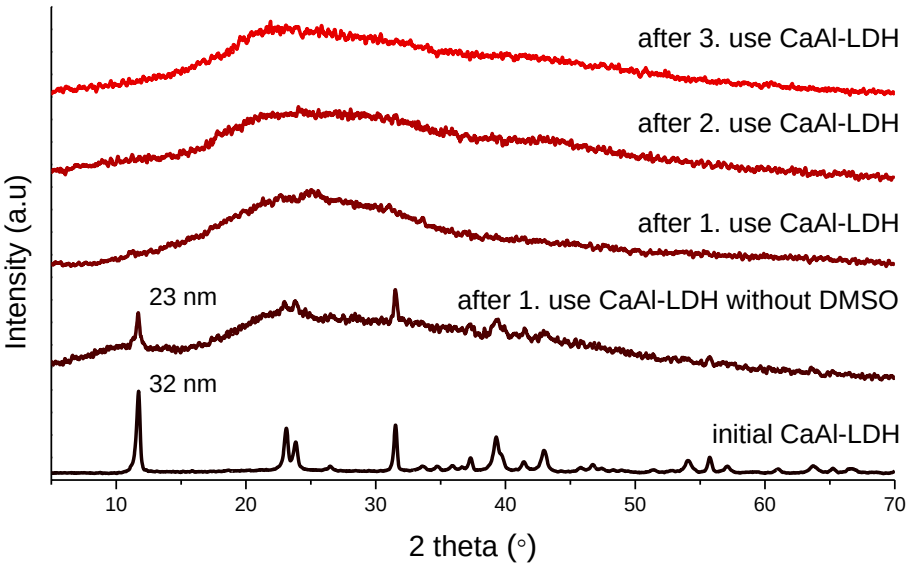

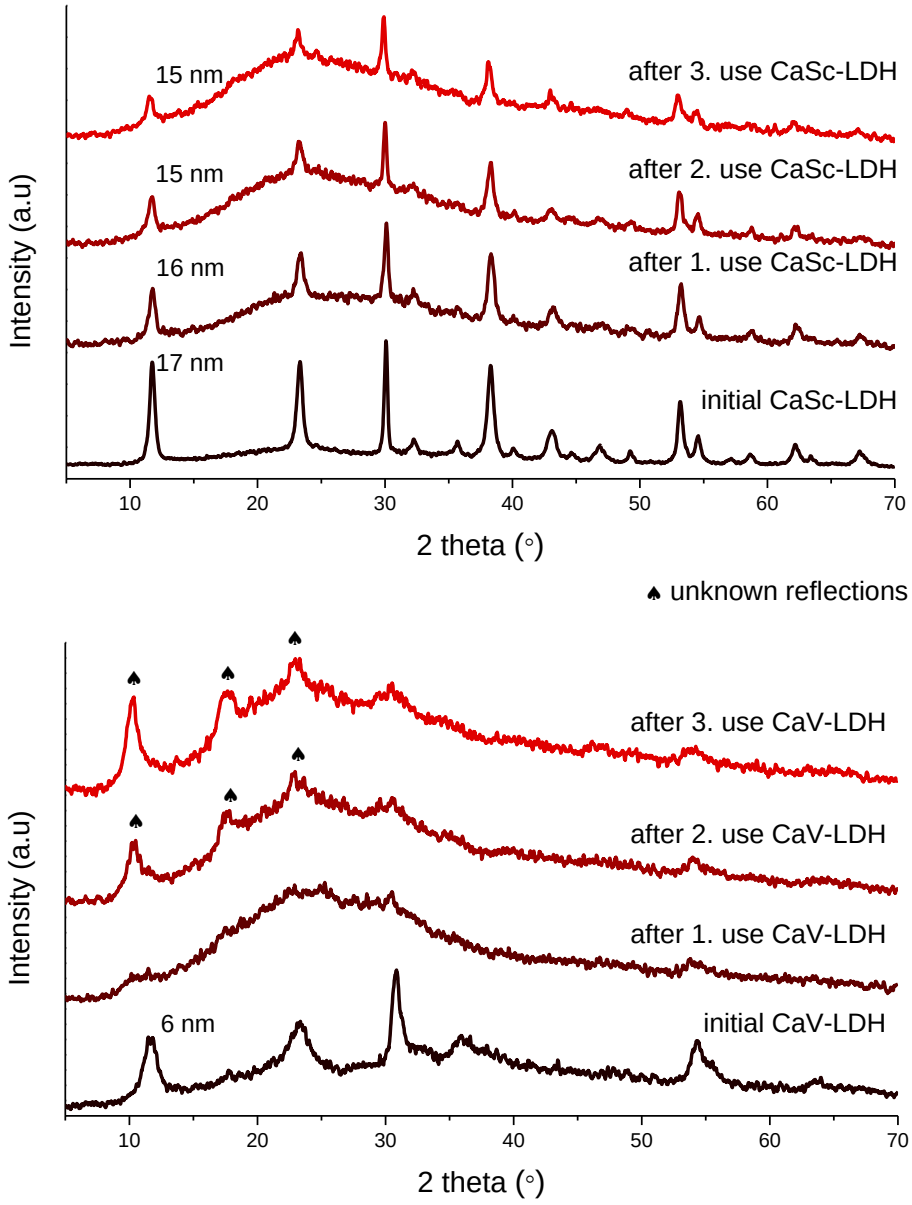
Intensity (a.u)
15 nm
after 3. use CaSc-LDH
15 nm
after 2. use CaSc-LDH
16 nm
after 1. use CaSc-LDH
17 nm
initial CaSc-LDH
10
20
30
40
50
60
70
2 theta (°)
♠ unknown reflections
Intensity (a.u)
after 3. use CaV-LDH
after 2. use CaV-LDH
after 1. use CaV-LDH
6 nm
initial CaV-LDH
10
20
30
40
50
60
70
2 theta (°)

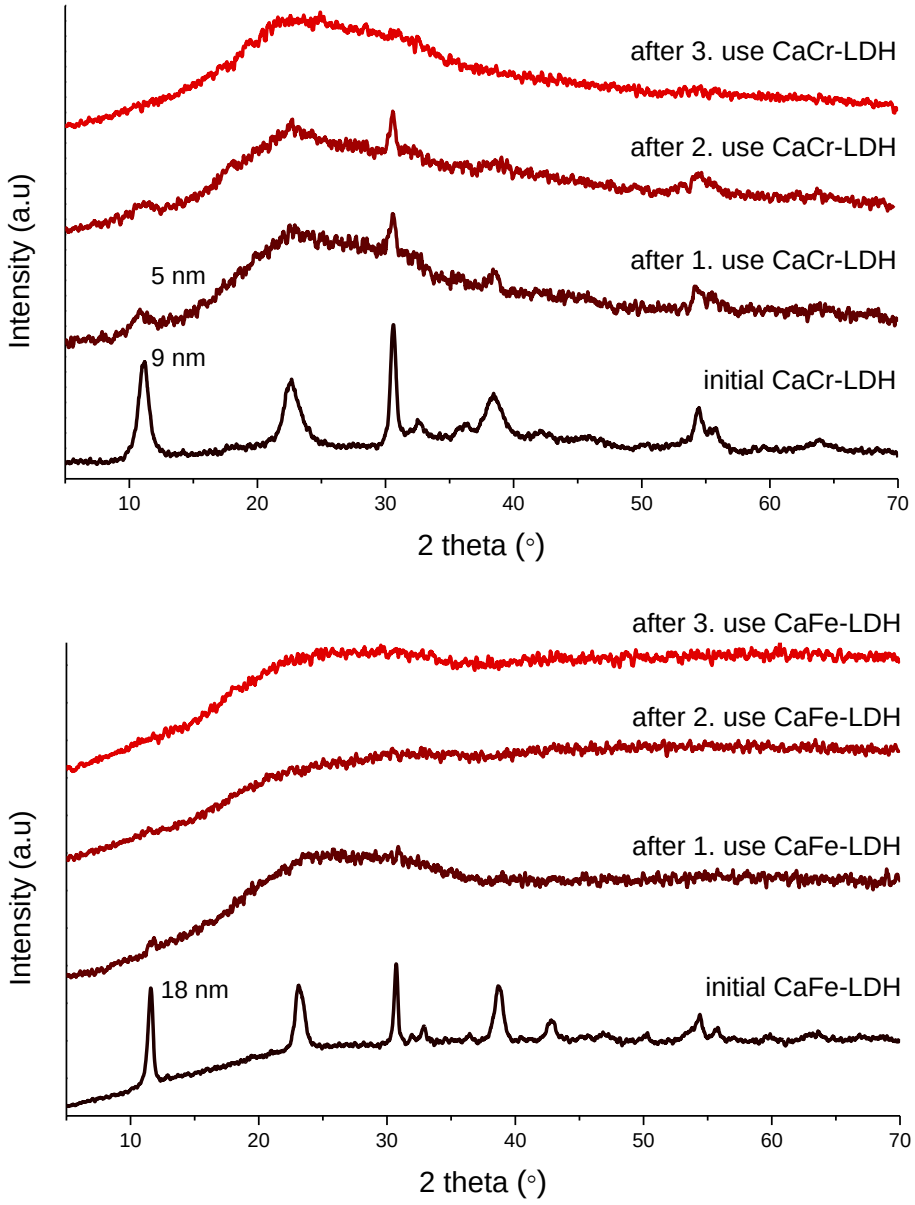
after 3. use CaCr-LDH
after 2. use CaCr-LDH
after 1. use CaCr-LDH
5 nm
9 nm
initial CaCr-LDH
Intensity (a.u)
10
20
30
40
50
60
70
2 theta (°)
after 3. use CaFe-LDH
after 2. use CaFe-LDH
after 1. use CaFe-LDH
18 nm
initial CaFe-LDH
Intensity (a.u)
10
20
30
40
50
60
70
2 theta (°)

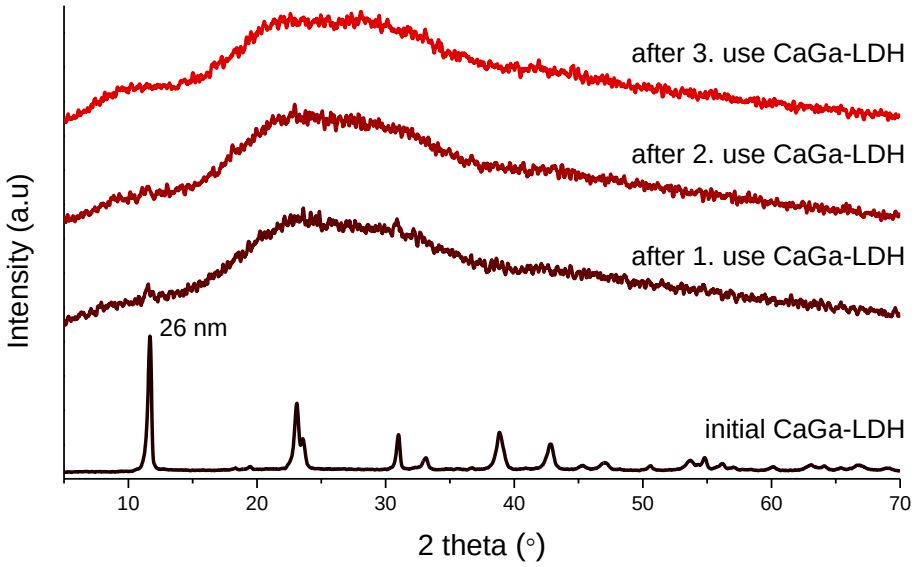
after 3. use CaGa-LDH
after 2. use CaGa-LDH
after 1. use CaGa-LDH
26 nm
initial CaGa-LDH
Intensity (a.u)
10
20
30
40
50
60
70
2 theta (◦)

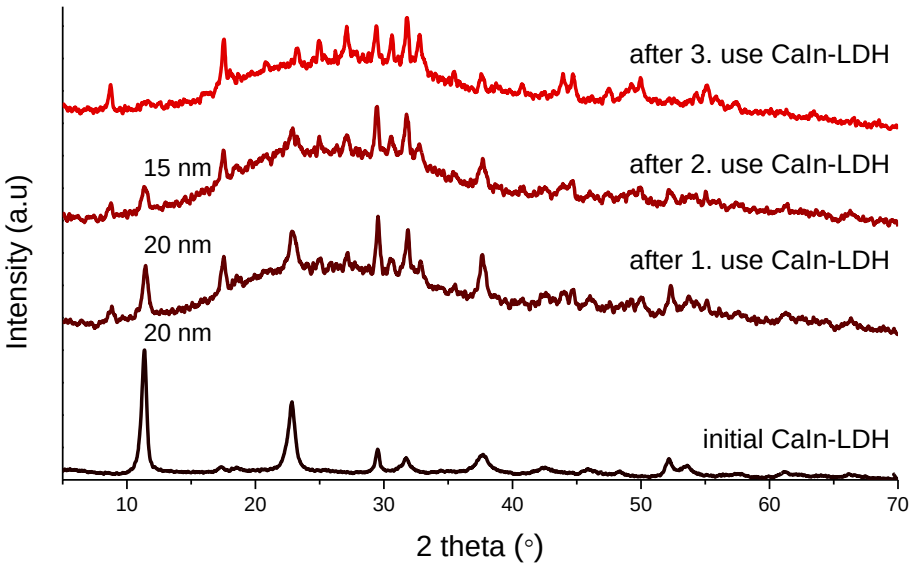
after 3. use CaIn-LDH
15 nm
after 2. use CaIn-LDH
20 nm
after 1. use CaIn-LDH
20 nm
initial CaIn-LDH
Intensity (a.u)
10
20
30
40
50
60
70
2 theta (◦)

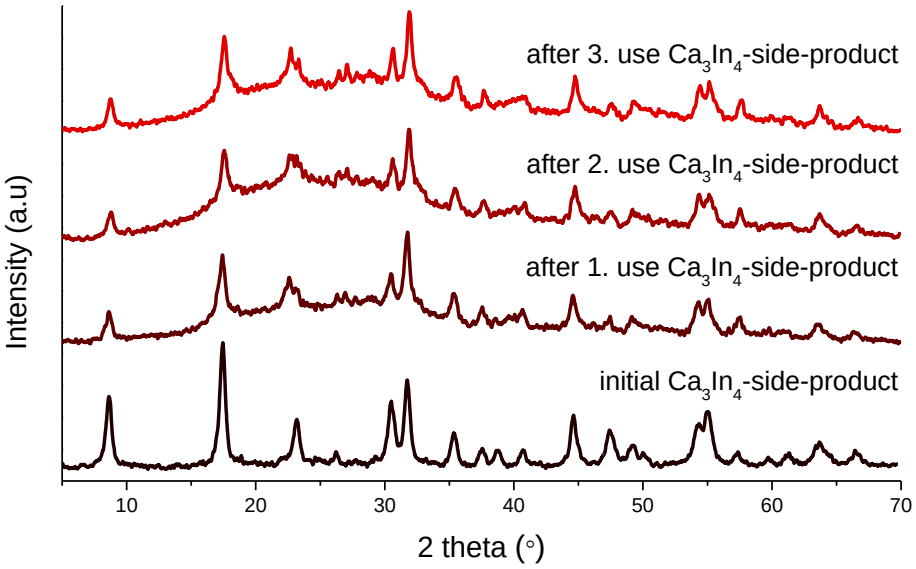

Fig. S11 X-ray powder diffraction curves of the initial, the used hydrocalumites and the Ca_3In_4-side-product.

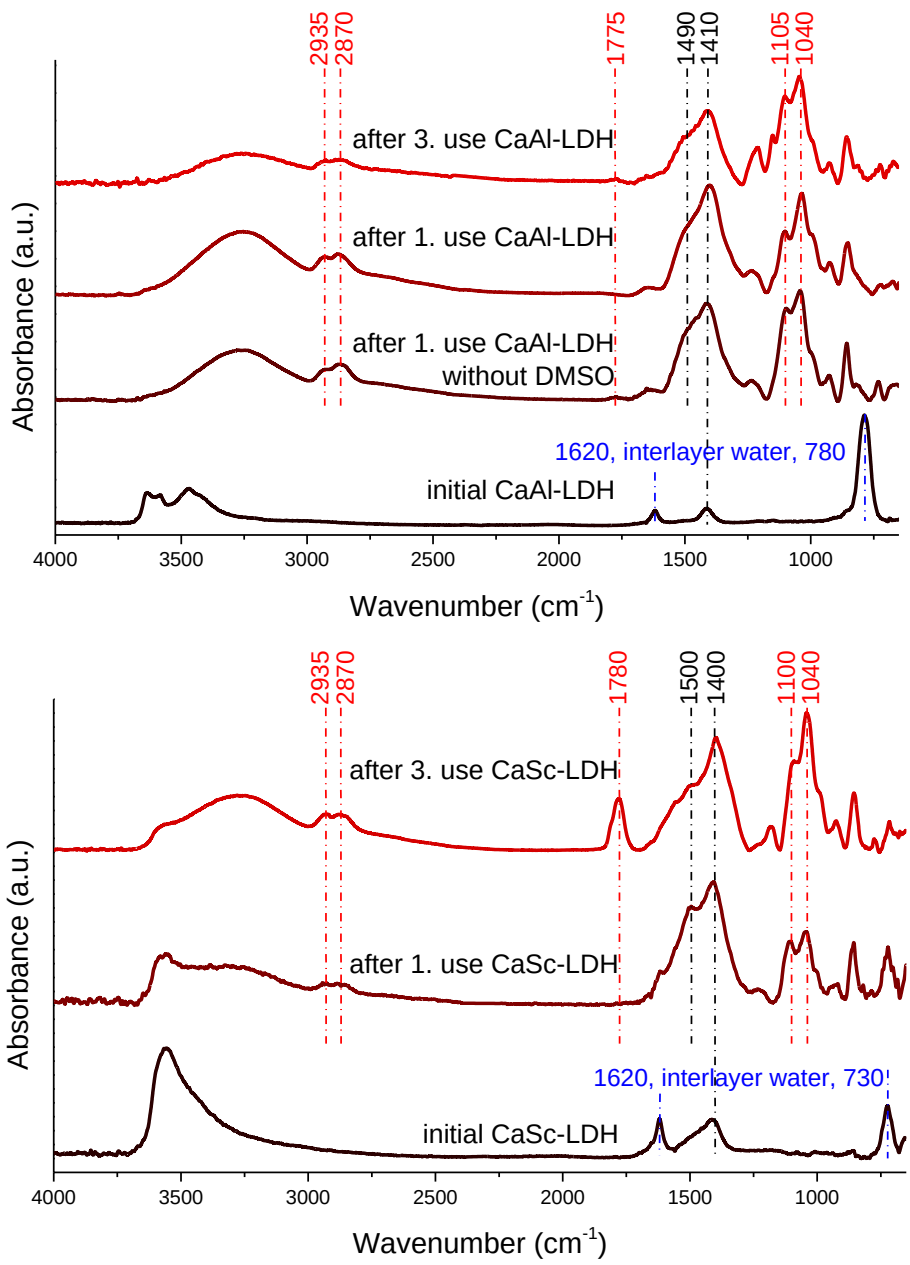
2935
2870
1775
1490
1410
1105
1040
after 3. use CaAl-LDH
after 1. use CaAl-LDH
after 1. use CaAl-LDH
without DMSO
1620, interlayer water, 780
initial CaAl-LDH
Absorbance (a.u.)
4000
3500
3000
2500
2000
1500
1000
Wavenumber (cm-1)
2935
2870
1780
1500
1400
1100
1040
after 3. use CaSc-LDH
after 1. use CaSc-LDH
1620, interlayer water, 730
initial CaSc-LDH
Absorbance (a.u.)
4000
3500
3000
2500
2000
1500
1000
Wavenumber (cm-1)

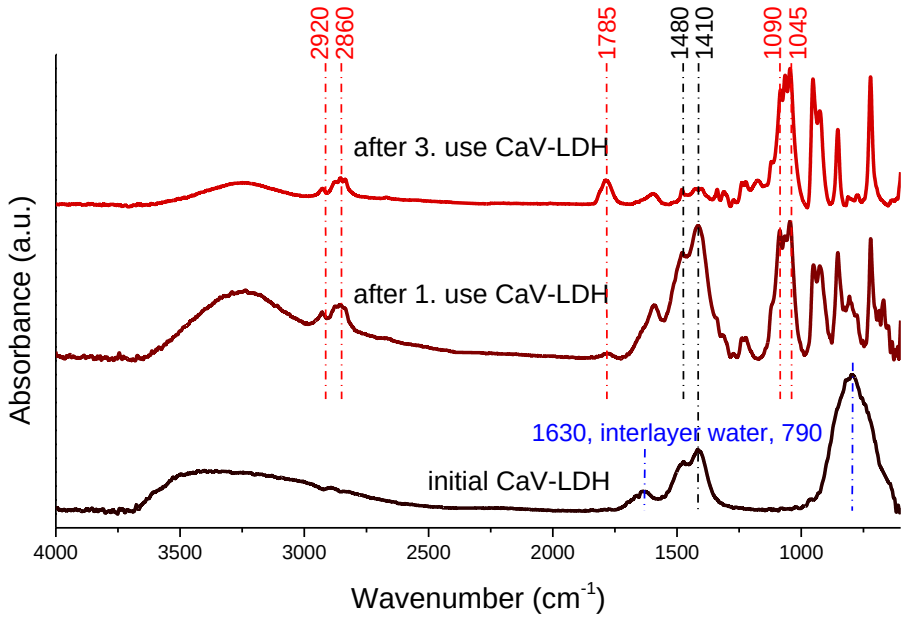
2920
2860
1785
1480
1410
1090
1045
after 3. use CaV-LDH
after 1. use CaV-LDH
1630, interlayer water, 790
initial CaV-LDH
Absorbance (a.u.)
4000
3500
3000
2500
2000
1500
1000
Wavenumber (cm-1)

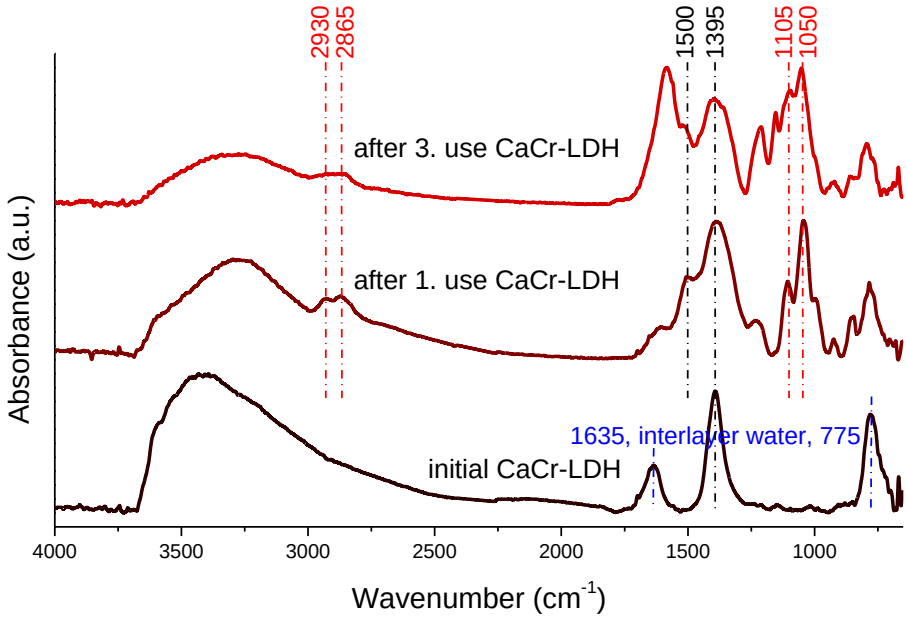
2930
2865
1500
1395
1105
1050
after 3. use CaCr-LDH
after 1. use CaCr-LDH
1635, interlayer water, 775
initial CaCr-LDH
Absorbance (a.u.)
4000
3500
3000
2500
2000
1500
1000
Wavenumber (cm-1)

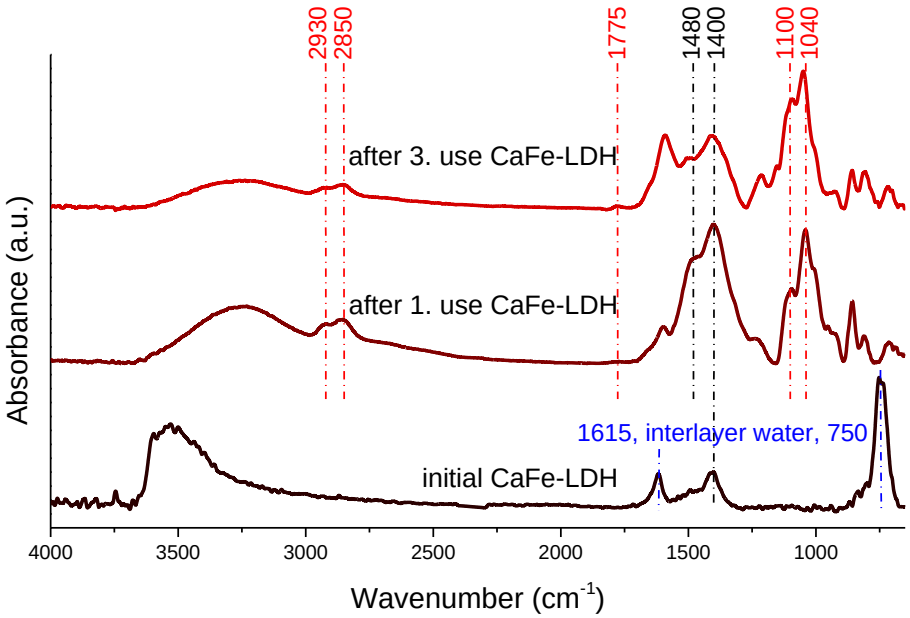
2930
2850
1775
1480
1400
1100
1040
after 3. use CaFe-LDH
after 1. use CaFe-LDH
1615, interlayer water, 750
initial CaFe-LDH
Absorbance (a.u.)
4000
3500
3000
2500
2000
1500
1000
Wavenumber (cm-1)

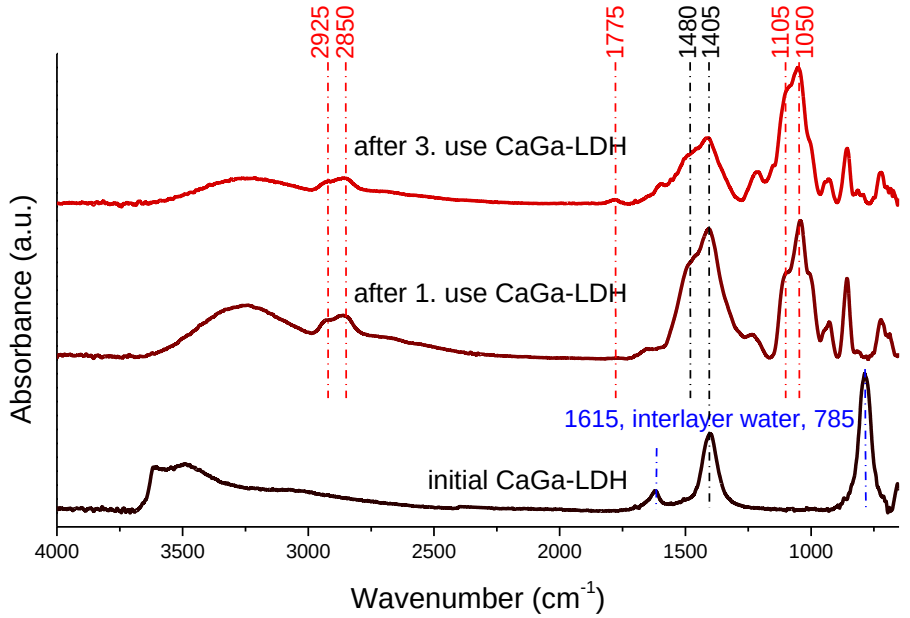
2925
2850
1775
1480
1405
1105
1050
after 3. use CaGa-LDH
after 1. use CaGa-LDH
1615, interlayer water, 785
initial CaGa-LDH
Absorbance (a.u.)
4000
3500
3000
2500
2000
1500
1000
Wavenumber (cm-1)

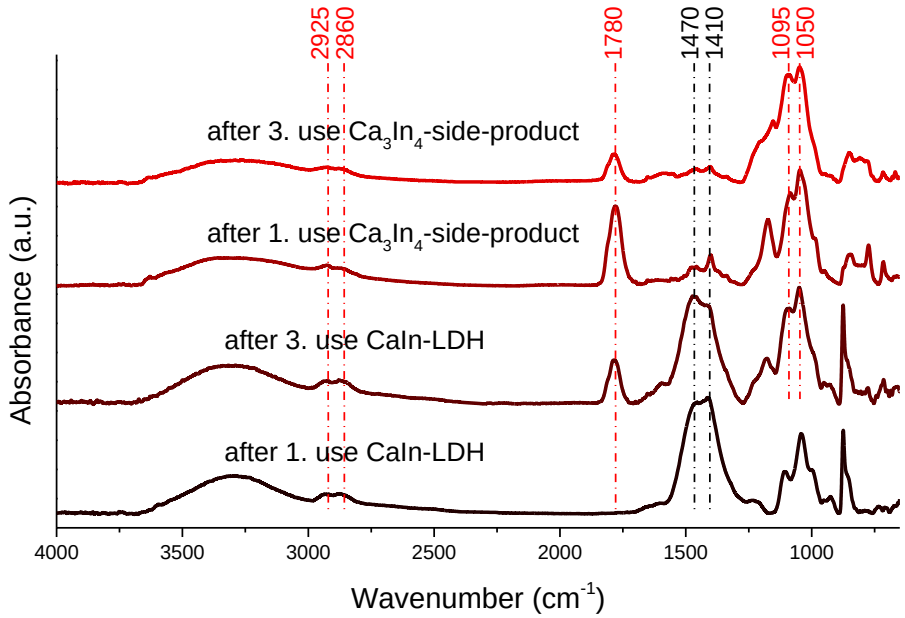

Fig. S12 Infrared spectra of the initial, the used hydrocalumites and the Ca_3In_4-side-product.

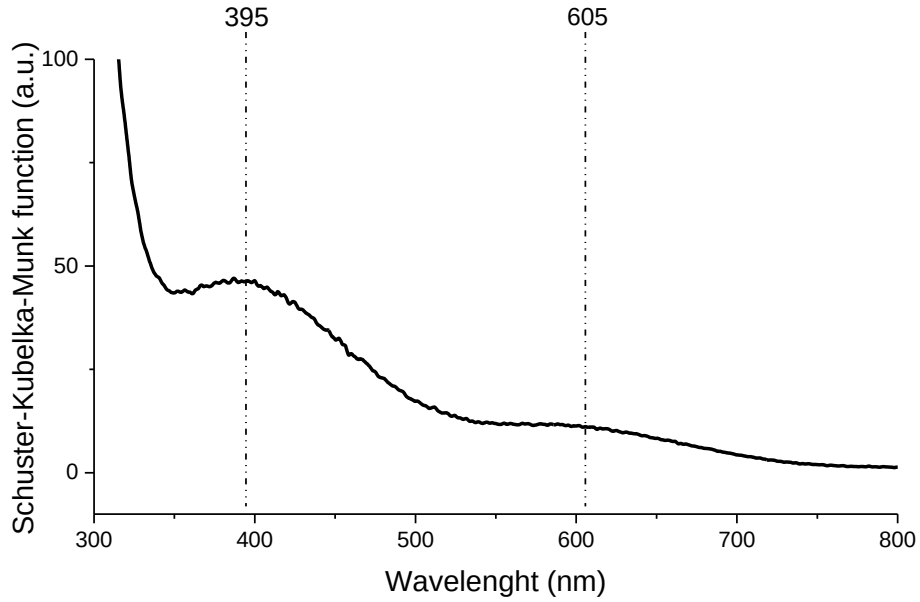

Fig. S13 UV–Vis diffuse reflection spectrum of the CaV-LDH.

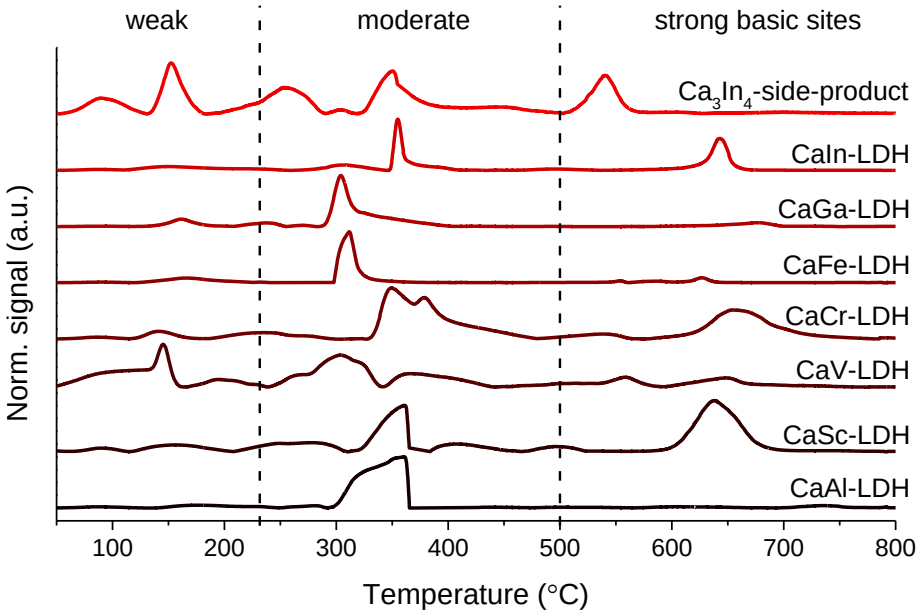

Fig. S14 CO_2-TPD profiles of the hydrocalumites and the Ca_3In_4-side-product.

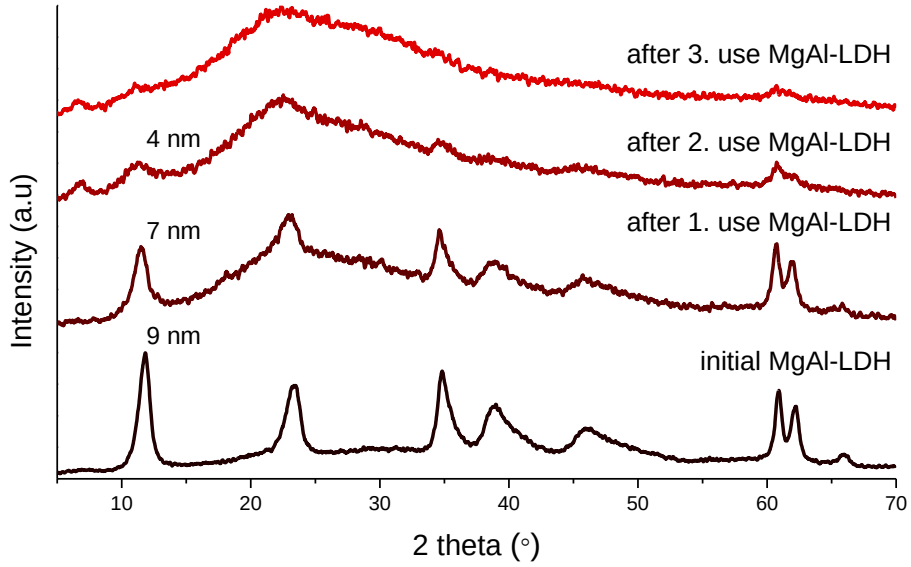
after 3. use MgAl-LDH
4 nm
after 2. use MgAl-LDH
7 nm
after 1. use MgAl-LDH
9 nm
initial MgAl-LDH
Intensity (a.u)
10
20
30
40
50
60
70
2 theta (◦)

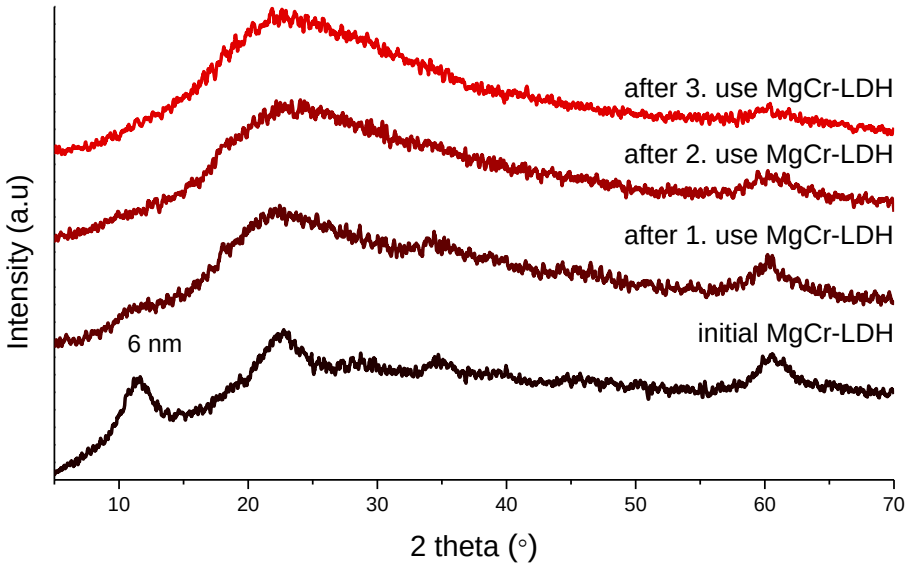
after 3. use MgCr-LDH
after 2. use MgCr-LDH
after 1. use MgCr-LDH
6 nm
initial MgCr-LDH
Intensity (a.u)
10
20
30
40
50
60
70
2 theta (◦)

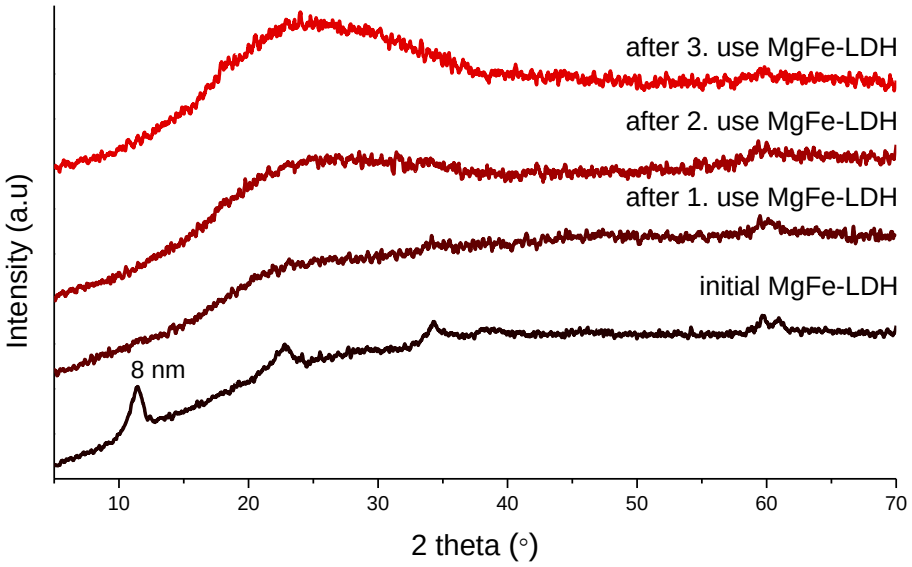
after 3. use MgFe-LDH
after 2. use MgFe-LDH
after 1. use MgFe-LDH
initial MgFe-LDH
8 nm
Intensity (a.u)
10
20
30
40
50
60
70
2 theta (◦)

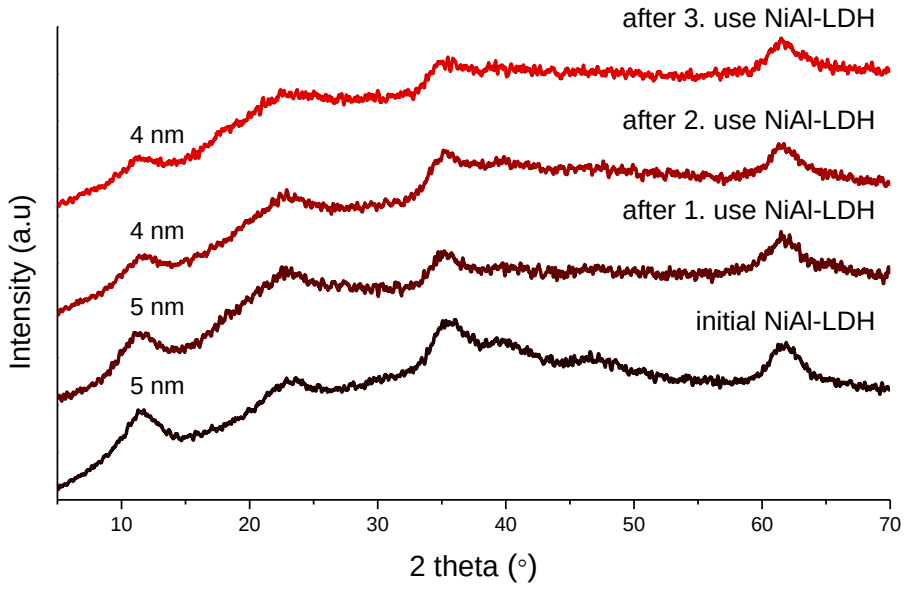
after 3. use NiAl-LDH
after 2. use NiAl-LDH
after 1. use NiAl-LDH
initial NiAl-LDH
4 nm
4 nm
5 nm
5 nm
Intensity (a.u)
10
20
30
40
50
60
70
2 theta (◦)

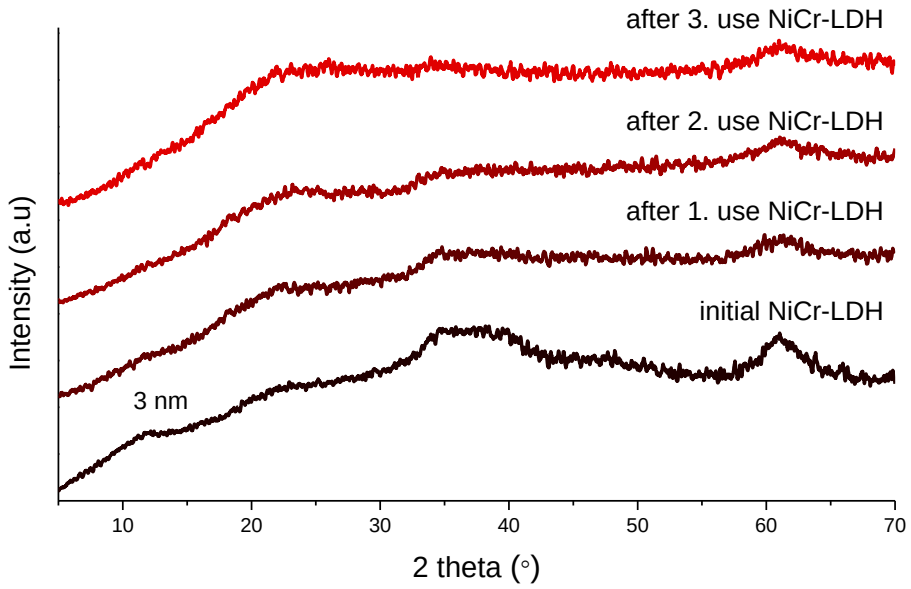
after 3. use NiCr-LDH
after 2. use NiCr-LDH
after 1. use NiCr-LDH
initial NiCr-LDH
3 nm
Intensity (a.u)
10
20
30
40
50
60
70
2 theta (◦)

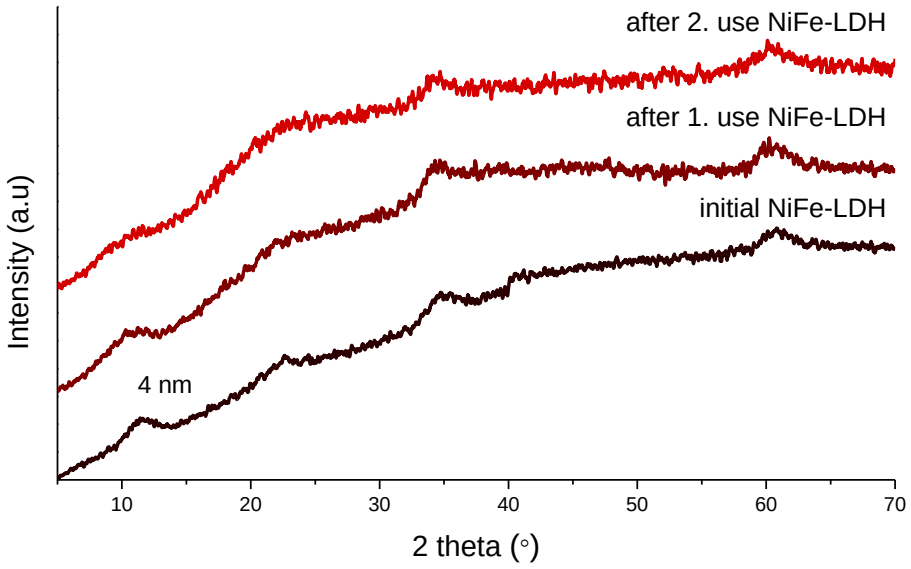
after 2. use NiFe-LDH
after 1. use NiFe-LDH
initial NiFe-LDH
4 nm
Intensity (a.u)
10
20
30
40
50
60
70
2 theta (◦)

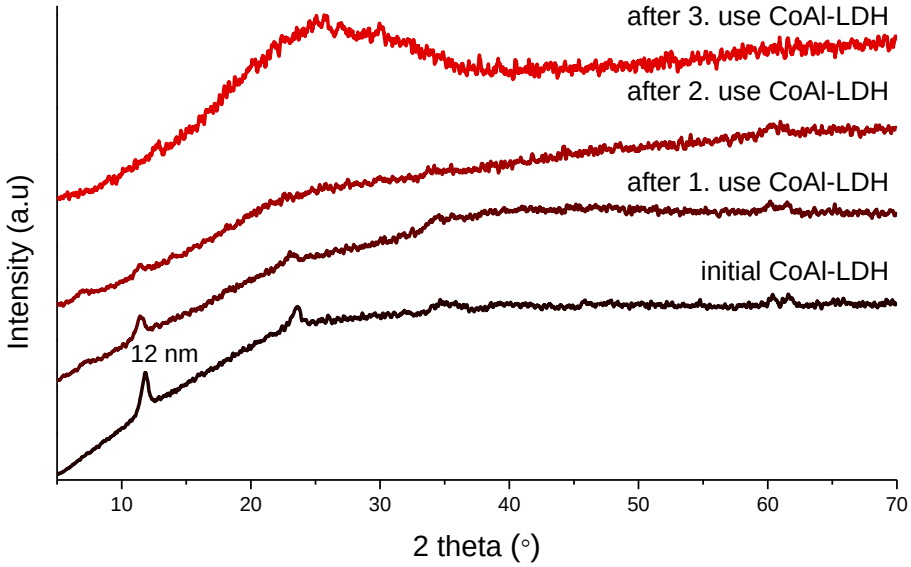
after 3. use CoAl-LDH
after 2. use CoAl-LDH
after 1. use CoAl-LDH
initial CoAl-LDH
12 nm
Intensity (a.u)
10
20
30
40
50
60
70
2 theta (◦)

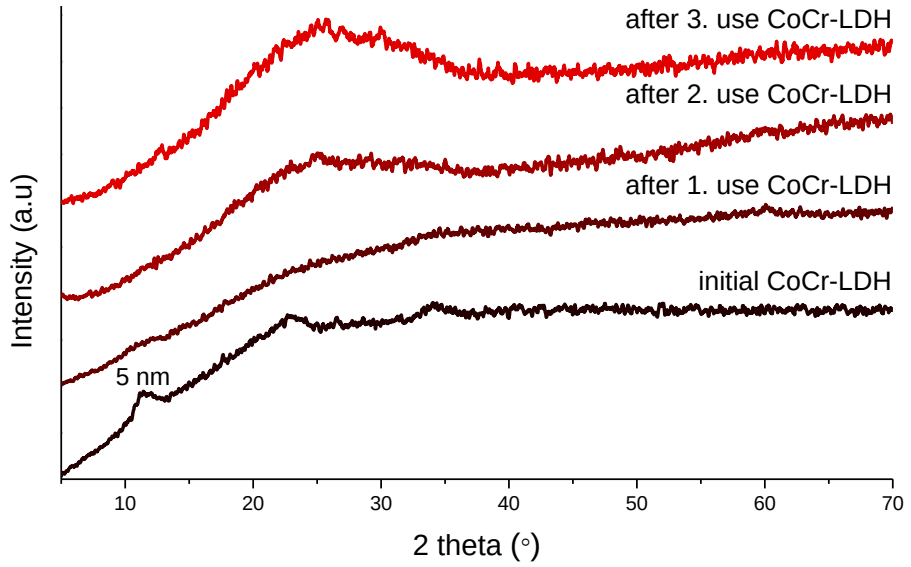
after 3. use CoCr-LDH
after 2. use CoCr-LDH
after 1. use CoCr-LDH
initial CoCr-LDH
5 nm
Intensity (a.u)
10
20
30
40
50
60
70
2 theta (◦)

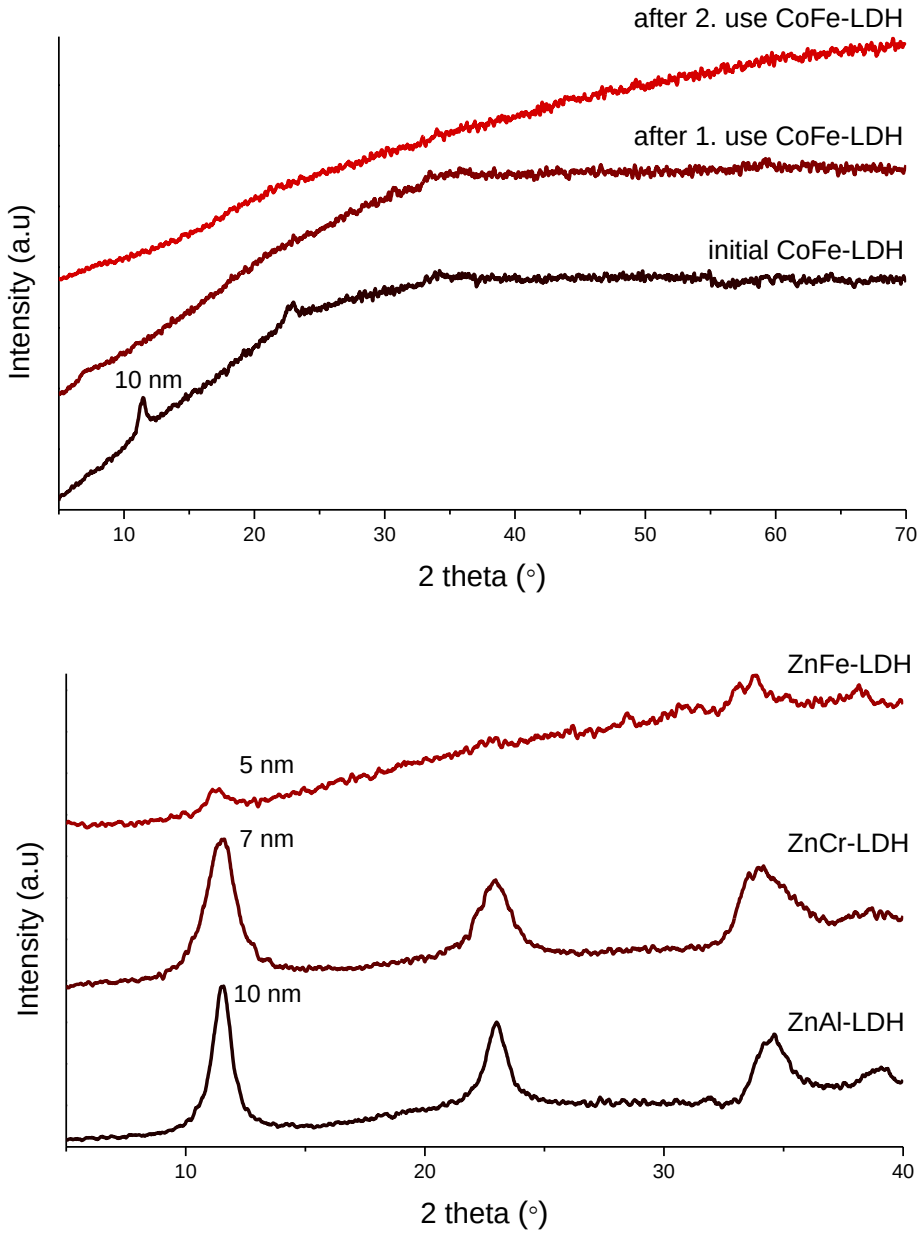

Fig. S15 X-ray powder diffraction patterns for the initial and used hydrotalcites.